The SARTOM Project;
Tomography for enhanced target detection for foliage penetrating airborne SAR

Ralf Horn[1], Armando Marino[2], Matteo Nannini[1],
Nick Walker[3], Iain Woodhouse[2]

1. German Aerospace Center (DLR)
2. University of Edinburgh
3. eOsphere Limited

Abstract

The SARTOM project addresses a key area of defence interest, namely the detection and identification of targets hidden in foliage. The project has provided a rich source of data obtained from a series of flight trials that were conducted in September 2006 at the test site Dornstetten, west of Munich, Germany. This multi-frequency (X-, C- and L-Band) and fully polarimetric data set is being examined with the use of advanced processing techniques designed to extract the maximum amount of information contained in the data: namely SAR Tomography and the analysis of multi-polarimetric and multi-frequency scattering characteristics of the foliage and target signatures. In supporting work a foliage radar penetration simulation model (PRIS) is being used to assess the detection and classification capabilities of different radar configurations applied to targets beneath foliage. In this paper results are presented derived from the experimental data and from the simulation model.

1. Introduction

The SARTOM project employs and is assessing the value of a range of advanced research techniques to the subject of foliage penetrating radar for the detection and classification of military targets; namely SAR Tomography, multi-polarimetric and multi-frequency systems and Polarimetric Interferometric SAR (PolinSAR).

During the first year of the project, 2006-7, an airborne campaign was conducted with the DLR E-SAR system which successfully obtained X-, C- and L-Band data over a range of targets for tomography, polarimetric, interferometric and multi-frequency analysis. (For bureaucratic reasons it was not possible to collect data at P band.)

Subsequent analysis has shown that the data collected is of a very high quality, which is proving to be a very valuable resource.

In Sections 2-4 in this paper we present a description of the Polarimetric SAR Tomography technique and the results obtained to date. In Sections 5-7 we present a summary of the PRIS modelling technique and show how this has been used to simulate a forest canopy with characteristics as measured from the experimental trials.

In Section 8 we derive some conclusions from the results so far and summarise the key areas we plan to address in the 3rd and final year of the project.

2. Polarimetric SAR tomography

SAR tomography [1] is an imaging technique that allows a vertical resolution through the construction of a synthetic aperture (tomographic aperture) in the direction perpendicular to the flight path. Hence, separation of multiple phase centres within a resolution cell becomes possible,

leading to a three-dimensional (3D) representation of the scene. SAR tomography is generally performed after standard 2D SAR processing. However, super-resolution methods deriving information from direction of arrival (DOA) approaches are often used to achieve high resolution and ambiguity rejection with a reduced number of observations.

SAR polarimetry studies the properties of the scatterers present in an observed scene that return a significant signal to the radar. By analysing different polarimetric combinations it is possible to derive information concerning the main scattering mechanisms related to a target and consequently to characterize it through its signature. In particularly, by carrying out a change of basis from the lexicographic (measured by the radar) to the "Pauli basis", it is possible to obtain a three element vector: (monostatic case) that detects for: odd-bounce (Pauli1), even-bounce (Pauli2), volumetric contributions (Pauli3).

The objective of this section is to describe how to obtain a 3D characterization of the scattering mechanisms of the observed scene. The theory is applied on real data acquired with DLR's E-SAR system over Dornstetten (Germany). The targets of interest are two trucks; one of them is outside the forest and the other is hidden beneath it.

Different target properties can be determined depending on the processing methods used to perform tomography. There are two main classes of tomographic processing: coherent and incoherent. We shall see that a combination of the two is necessary to derive the maximum amount of information. On the one hand, coherent processing methods like the time domain beamforming (TDB) [2] allows the combination of all the polarimetric information in one single colour-coded tomogram, due to its linearity, leading to the determination of a signature of the viewed target. On the other hand, the use of incoherent methods like the Capon beamformer [3] is necessary to overcome the resolution and ambiguity rejection limitations of the TDB.

Details on the TDB algorithm and the Capon beamformer concerning tomography can be found in [2, 3].

3. Experimental results

In this section some results obtained on real data are presented. First of all results obtained by means of the TDB are presented in Figure 1, which shows a truck hidden under foliage.

It can be seen that the backscattered power of Pauli3 (HV) in correspondence to the target has no significant amplitude when compared with the Pauli1 and Pauli2 components. The truck is represented by the yellow spot located under the canopy that corresponds precisely to the combination of Pauli1 and Pauli3 components.

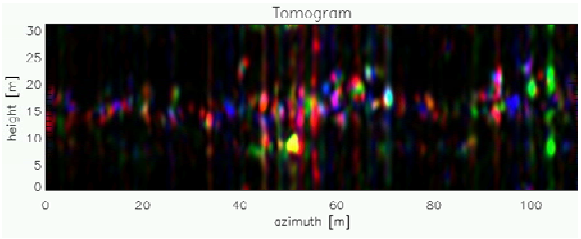

Figure 1. Colour coded polarimetric tomogram in the Pauli basis of the hidden truck by means of the TDB algorithm. R=Pauli1, G=Pauli2, B=Pauli3. The presence of a sufficiently dense forest filters the Pauli3 component allowing the identification of the target by means of strong odd-, even-bounce reflection. The hidden truck is represented by the yellow spot at approximately 52 metres in azimuth.

The tomographic results generated by means of the Capon beamformer, for the same target, are presented in Figure 2. It is interesting to note that the polarimetric combinations cannot be represented in one single colour coded image because of the non-linearity of the function. For this incoherent processing algorithm the images

in the lexicographic basis have been combined before the tomographic SAR processing to obtain the Pauli tomograms.

The canopy and the ground contributions are represented with their detailed structure. In comparison with the TDB algorithm the Capon beamformer achieves higher resolution. By examining the hidden truck, one can observe the relative differences between the polarimetric responses. The target is visible in all the polarization channels and combinations except the cross-polarized one (HV). This main difference can be related to the high density of the canopy over the truck. This causes a weaker cross-polarized contribution to reach the target (in comparison with the co-polarized channels) because of the attenuation that HV suffers from volumetric structures.

It is interesting to observe that different polarizations detect different parts of the truck (e.g. Pauli1 is more sensitive to the rear part of it, while Pauli2 is more sensitive to the front of it).

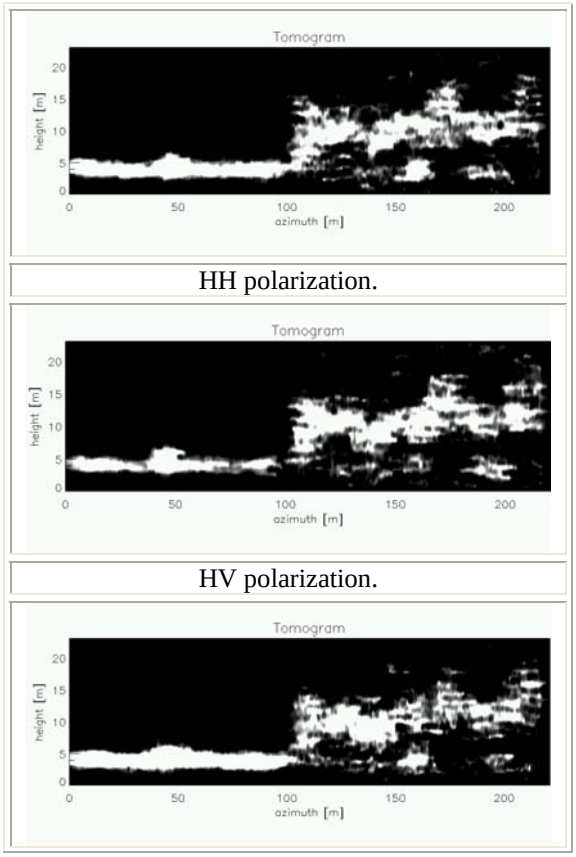

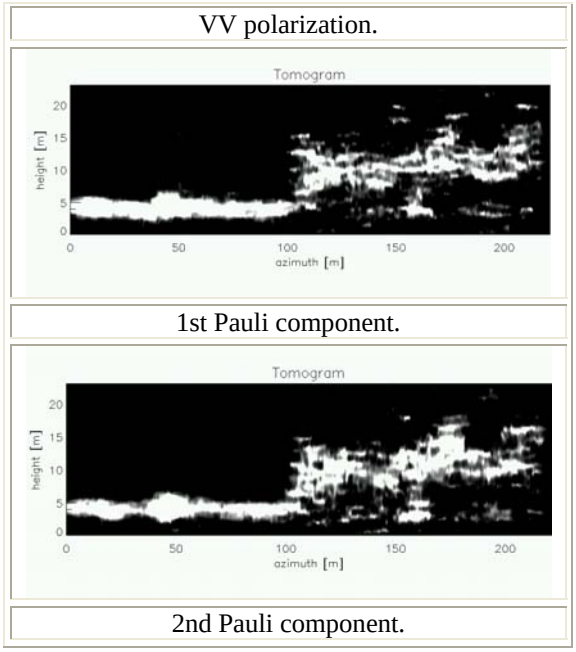

Figure 2. Polarimetric tomograms of the trucks obtained by means of the Capon beamformer. The ground and canopy contributions are visible in each case.

4. Target (truck) height estimation

By observing the tomograms shown in Figure 2 and focusing on the target's contribution, it is possible to associate a range of heights where the response of the target is not negligible. In this way an estimate of the height of the target can be made. Considering an azimuth interval where the target response is present, averaging the tomogram's response a pseudo-power backscattering profile of the truck can be obtained. From this process the diagrams shown in Figure 3 are generated. From Figure 3 a minimum and a maximum height for the truck and the forest can be determined. The black dots indicate the boundary height of the two structures. The target's actual height is 3m and the estimated one is 2.3m. The bottom height of the truck is estimated from the HH polarization, while the top is estimated from the Pauli2 response.

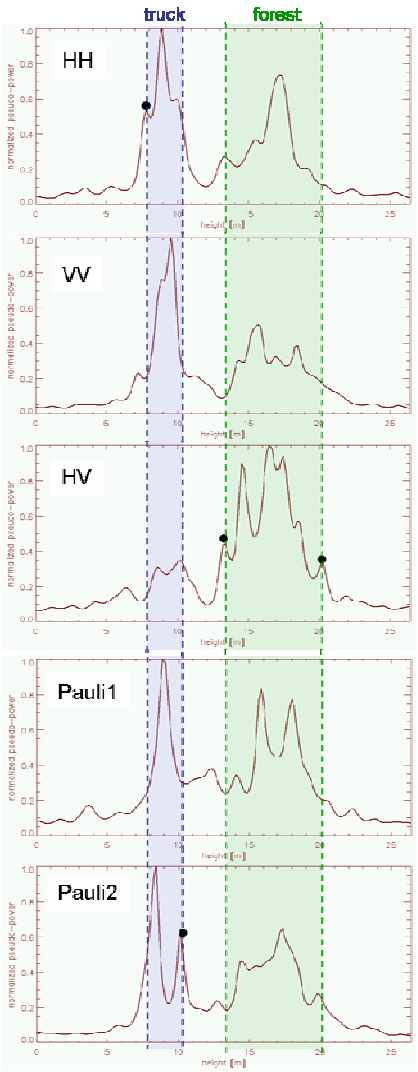

Figure 3. Tomographic averaged profile of the hidden target. Due to the different polarimetric responses it is possible to estimate the height of the truck in 2.3m. The actual height is 3m.

Due to the complex structure of the target it is not possible to uniquely match the location of the estimated phase centres (what the sensor actually sees) with a corresponding location on the target. However, obtaining the same order of magnitude for the estimate and the actual height is encouraging for further investigations.

In order to demonstrate the reliability of this analysis, the boundary height estimation has been carried out also for the canopy. The polarimetric channel that is more sensitive to volumetric structures is the cross-polarized channel HV (neglecting the scaling factor it corresponds to the Pauli3 component). Hence, this component should allow the closest forest height difference estimation. Indeed, examining the HV averaged tomogram it is possible to see that it detects for the minimum and the maximum height of the canopy over the truck and in agreement with the theory.

5. PRIS (Polarimetric Radar Interferometric Simulator)

Calculating the radar SAR backscatter from a forest environment is generally hard to achieve, mainly due to the high heterogeneity of the vegetation layer (composed by leaves, branches, trunks, etc). Forest elements can, of course, vary in dimension, shape, orientation and electrical characteristics.

A backscattering simulator is a valuable tool for studying the SAR return from forest, allowing the separation of the different scattering mechanisms and consequently the possibility to perform sensitivity analysis for the forest parameter of interest.

However, the computational effort of a coherent full wave simulation is generally not feasible, especially when the aim is to perform a sensitivity analysis, requiring multiple runs of the algorithm. In this context, a simplification of the problem is needed. The radiative transfer (RT) equation is one way to achieve this aim. A systematic explanation of the advantages of the different techniques is given by [4] and [5].

6. Simulation of a corner reflector beneath the forest canopy

PRIS is an interferometric RT model, which simulates a pair of complex backscatter images from a 3-D forest.

Two main steps are necessary in order to perform the backscattering simulation of a forest scene: firstly, the 3-D forest is constructed; secondly, the interferometric

and polarimetric backscattering from the simulated scene is calculated.

For the first step, information about the forest stand is required. The forest is a composite environment, with different characteristics depending on the type of forest; hence a ground truth campaign must be conducted to ensure that the modelled forest has similar characteristics to the forest under consideration. In general we are not interested in the simulation of exact specific scenarios. Instead we are interested in the overall statistical description of the forest characteristics, so we can study the electromagnetic behaviour with a sensitivity analysis. In this case knowledge about individual trees is superfluous, and a mean description of the forest is sufficient. PRIS is able to input both exact and approximate information about the forest scenarios. However in this paper the simulation will be carried out by the use of averaged information.

The microwave frequency selected for the simulation is L. The reason of this choice is related with the penetration capability of the 24 cm wavelength radiation. The sensor resolution is 1 x 2 m (azimuth x range) and the baseline is 10 m (the selection of these values is related with the SARTOM dataset presented in the previous sections). The look angle is 45 degree. However, it is possible to carry out simulation with other angles, for example including a much steeper look angle (e.g. 70 degree).

Figure 4. A schematic representation of trees in the simulated stand forest. The point brightness is related with the amount of tree crown. (PRIS)

Figure 4 shows the location of the trees in the simulated forest stand (please note, it is not a SAR image). The pixel brightness corresponds to the amount of vegetation in the crown.

In order to have an idea about the attenuation effect of the foliage we simulate a classical FOLPEN (FOLiage PENetration [6]) experiment locating a trihedral corner reflector (triangle base of 1.49 m) in the forest stand, beneath the canopy. In this way, the results are immediately comparable with the real experiment (as described in Section 7).

The second simulation step considers the calculation of the polarimetric backscattering for two images acquired from two slightly different look angles. The single tree crown is modelled as a random volume (RVoG: [7, 8]) although with a 3-D crown shape parameterised from ground data and allometric relationships (allometry is the science studying the differential growth rates of the parts of a living organism's body part or process [9]).

The crown volume is modelled as comprising randomly distributed elements with statistically homogeneous scattering and extinction properties. The response from the ground beneath the canopy is calculated by a rough surface model that takes into account soil roughness and moisture[10]. Moreover, the trunk backscattering contribution is evaluated considering the trunk-ground double-bounce effect [11]. Finally, the corner reflector return is calculated as an ideal triangular trihedral corner reflector (CR), hence its theoretical backscatter cross-section is equal to $4\pi a^4/3\lambda^2$ [12], where a is the base of the triangle.

7. Results and Comparison with real data

The results simulated by the PRIS model are compared with the data set acquired during the SARTOM campaign 2006 [13]. The simulated test area is located by the trihedral corner reflector (1.49 m) named CR04, beneath the canopy. The L-band fully-polarimetric and interferometric (baseline 10 m) SAR data are used. The same sensor characteristics are set in PRIS.

Figure 5 shows the backscattering response for HH, VV and HV polarisations. In order to compare the polarimetric features of the real and simulated data, we have plotted in Figure 6 the backscattering amplitude for the simulated and real data along a range-line passing for the CR.

It is important to note that the y-axes scales for the two columns are not comparable, because the two results can differ for a factor depending on the signal processing of the raw data. For this reason, a comparison of the scale value is meaningless; instead we compare the ratio between the peaks associated with different backscattering components (i.e. the target over clutter peak amplitude ratio). The corner reflector is located around ground pixel 57 in the simulated data and 54 in the real data.

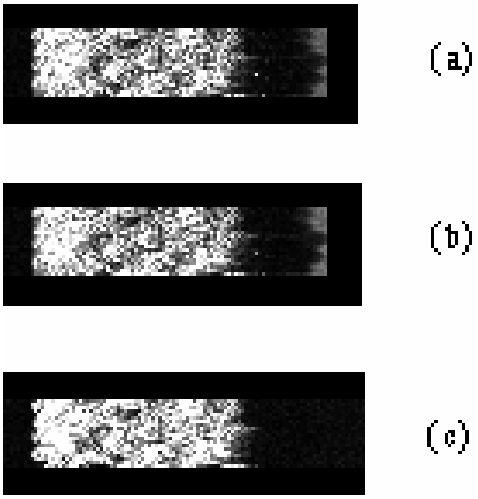

Figure 5. Simulated backscattering images for (a) HH, (b) VV and (c) HV polarisations. (PRIS)

As expected, the co-polarisations (HH and VV) have a strong peak in the location of the CR (for both simulated and real data). The other peaks in the co-polarised returns are mainly associated with the trunk-ground double-bounces. In particular HH has the strongest contributions (i.e. Brewster angle). The ratio between CR peak and clutter in the HH images is 2.28 for the simulated data and 2.36 for the real data.

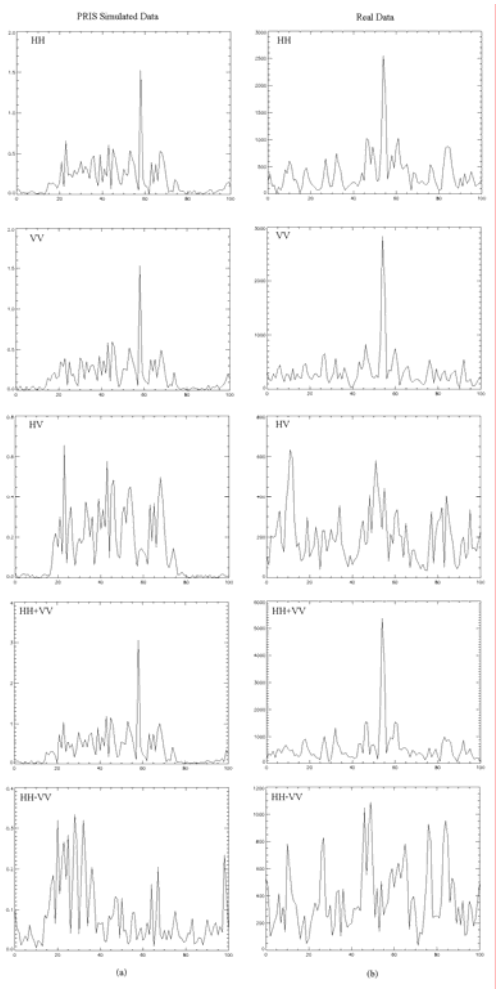

Figure 6. Backscattering of a range line passing for the CR. (Left hand side) Simulated data; (right hand side) Real data.

However, the simulation results are strongly dependent on the particular forest realisation, as the location of the different trees and their dimension. As presented in the previous section, in PRIS the distribution of the trees within the simulated area and the individual plant dimensions are randomised. Moreover, in a heterogeneous environment (e.g. forest) the backscattering is strongly dependent on the particular position of the scatterers. Hence, the final backscattering can be significantly different from one simulation to another. However, the main characteristics shown here (i.e. peak to backround ratio) are relatively unvaried. To summarise, the ratio between CR and clutter peaks for the HH polarisation generally oscillates between 2

and 4, depending on the amount of covering for the CR.

The other plots in Figure 6 represent the three components of the Pauli scattering vector:

$$\text{Pauli } 1 = \frac{1}{2}(HH + VV),$$

$$\text{Pauli } 2 = \frac{1}{2}(HH - VV),$$

$$\text{Pauli } 3 = 2HV$$

[14], that are related with the physics of the scattering mechanisms.

It can be seen that the cross-polarisation HV has a return lower than the co-polarisations and it is quite uniformly distributed in all the forest. It is weakly sensitive to the CR and the trunks. This component observes mainly the forest background.

Pauli 2 is particularly receptive to the even-bounce scattering contributions (e.g. double-bounces). For this reason, in both of the plots the trunk returns are magnified and easy to detect. The trihedral CR is characterised by a triple-bounce response (i.e. not even-bounce), for this reason the return is much lower.

Pauli 1 is sensitive to the odd-bounces (e.g. surface backscattering, triple bounces), hence the trihedral CR return is magnified by this polarisation. In both the images the detectability of the CR is strongly increased (high separation from the clutter background).

In conclusion, the polarimetric information of target and clutter seem to be preserved, consequently detection and retrieval Pol-InSAR algorithms can theoretically run and be tested on PRIS.

Finally, Figure 7 shows the height retrieval using the phase centre for different polarisations (HH, VV and HV). As expected the HV polarisation gives a higher estimation because it is weaker sensitive to ground and trunks. The HH and VV polarisations are usually lower than HV, except where the canopy is exceedingly dense and the return from the bottom of the forest becomes too weak. In particular the HH is lower than VV in the presence of trunks (Brewster angle effect). In the simulation the corner reflector is placed at the ground distance position 2475 m and it is represented as a square point on the ground.

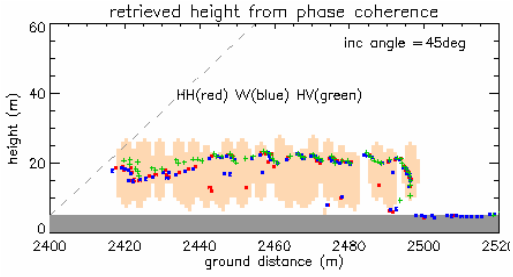

Figure 7. Forest cut in the ground range – height coordinates. Height retrieved by the use of the phase centre for HH, VV and HV polarizations. (PRIS)

8. Conclusion

Results obtained by means of polarimetric SAR tomography have been presented. The 3D polarimetric analysis completed with the TDB algorithm led to consistent and reliable results that can be exploited to define a signature of the hidden target for target detection purpose. The imaging advantages of the Capon beamformer and the possibility to deal with different measurements of the scene combining the lexicographic and Pauli basis, allowed to carry out the estimation of the height of the target hidden beneath foliage.

A robust method that couples the advantages of these two imaging techniques is part of the future work.

It has been shown that consistent results can be derived between the PRIS simulation algorithm and the results from the experimental trials. Modelling work is ongoing and includes the incorporation of models of realistic targets within the forest canopy. This will enable a more complete analysis of the radar parameter space (for example polarisation and frequency

combinations) that will best assist with the detection and classification of targets under foliage.

Acknowledgements

The work reported in this paper was funded by the Electro-Magnetic Remote Sensing (EMRS) Defence Technology Centre, established by the UK Ministry of Defence and run by a consortium of SELEX Galileo, Thales UK, Roke Manor Research and Filtronic.

References

[1] Reigber and A. Moreira, First Demonstration of Airborne SAR Tomography using multibaseline L-Band Data, IEEE Trans. on Geosc. and Remote Sensing Vol. 38, no.5, pp.2142-2152, 2000

[2] M. Nannini and R. Scheiber, A Time Domain Beamforming Algorithm for SAR Tomography, Proc. EUSAR conf., Dresden, 16-18 May, 2006A.G. Thomas, M.C. Berg, “Medium PRF set selection: an approach through combinatorics.”, *IEE Proc.-Radar, Sonar Navig.*,, Vol. 141, No. 6, December 1994, pp.307- 311

[3] F. Lombardini and A. Reigber, Adaptative spectral estimation for multibaseline SAR Tomography with airborne L-band data, in Proc. IGARSS, Toulouse, France, 2003

[4] M. A. Karam, A. K. Fung, R. H. Lang, and N. S. Chuahuan, "A microwave scattering model for layered vegetation," IEEE Transaction on Geoscience and Remote Sensing, vol. 30, pp. 799-808, 1992.

[5] S. S. Saatchi and K. C. Mcdonald, "Coherent effects in microwave backscattering models for forest canopies," IEEE Transaction on Geoscience and Remote Sensing, vol. 35, 1997.

[6] J. G. Fleishman, S. Ayasli, E. M. Adams, and D. R. Gosselin, "Foliage penetration experiment Part I: Foliage attenuation and backscatter analysis of SAR imagery," IEEE Transaction on Aerospace and Electronic Systems, vol. 32, 1996.

[7] R. N. Treuhaft, S. N. Madesen, M. Moghaddam, and J. J. Van Zyl, "Vegetation characteristics and underlying topography for interferometric radar," Radio Science, vol. 31, 1996.

[8] S. R. Cloude and K. P. Papathanassiou, "Polarimetric SAR interferometry," IEEE Transaction on Geoscience and Remote sensing, vol. 36, 1998.

[9] J. K. Niklas, Plant allometry: the scaling of form and process. Chicago: The University of Chicago Press, 1994.

[10] Y. Oh, K. Sarabandi, and F. T. Ulaby, "An empirical model and an inversion technique for radar scattering from bare soil surface," IEEE Transaction on Geoscience and Remote Sensing, vol. 30, pp. 370-381, 1992.

[11] J. A. Richards, G. Q. Sun, and D. S. Simonett, "L-band radar backscatter of forest stands," IEEE Transaction on Geoscience and Remote Sensing, vol. 25, pp. 487-498, 1987.

[12] I. H. Woodhouse, Introduction to Microwave Remote Sensing. London: Taylor and Francis, 2006.

[13] R. Horn, M. Nannini, and M. Keller, "SARTOM airborne campaign 2006 data acquisition report," 2006.

[14] S. R. Cloude and E. Pottier, "A review of target decomposition theorems in radar polarimetry," IEEE Transaction on Geoscience and Remote Sensing, vol. 34, 1996.